Journal of Computational Physics 272 (2014) 266–278

Contents lists available at ScienceDirect

Journal of Computational Physics

www.elsevier.com/locate/jcp

An operator expansions method for computing Dirichlet–Neumann operators in linear elastodynamics

Zheng Fang, David P. Nicholls *

Department of Mathematics, Statistics, and Computer Science, University of Illinois at Chicago, Chicago, IL 60607, United States

ARTICLE INFO

Article history:
Received 16 July 2013
Received in revised form 16 April 2014
Accepted 21 April 2014
Available online 28 April 2014

Keywords:
Linear elastodynamics
Boundary perturbation methods
Navier's equation
High-order spectral methods
Dirichlet–Neumann operators

ABSTRACT

The propagation of linear elastic waves arises in a wide array of applications, for instance, in mechanical engineering, materials science, and the geosciences. Many configurations of interest can be effectively modeled as layers of isotropic, homogeneous materials separated by thin interfaces across which material properties vary rapidly. In the frequency domain one must solve a system of coupled elliptic partial differential equations, however, this can be greatly simplified in the instance of layered media by considering interface unknowns. To realize this one must be able to produce normal stresses (tractions) at these interfaces and Dirichlet–Neumann Operators accomplish this. In this contribution we discuss a novel Boundary Perturbation approach to compute these operators in a rapid, high-order, and robust fashion.

1. Introduction

The propagation of linear elastic waves in an inhomogeneous medium arises in a wide array of applications, for instance, in mechanical engineering [2], materials science [20], and the geosciences [9,56]. These disturbances are governed by the wave equation where the velocity of propagation depends upon the properties of the material in question [1,2]. In many applications, e.g. in the instance of plane-wave incident radiation, it is sufficient to compute the scattering at a single temporal frequency and thus, in light of the linear nature of the governing equations, one may adopt the frequency-domain approach as we do here resulting in a system of elliptic PDE to be solved.

In many instances, the medium may be effectively modeled by two or more isotropic, homogeneous layers which are delineated by sharp interfaces across which the material properties vary rapidly. Furthermore, for many purposes these can be specified by graphs of (single-valued) functions which, additionally, are periodic. Many numerical algorithms have been devised for the simulation of this problem. The Finite Difference (FDM) [39,50], Finite Element (FEM) [29,61], and Spectral Element (SEM) [31,32] methods have been studied but suffer from the fact that they discretize the full volume of the model which not only introduces a huge number of degrees of freedom, but also raises the difficult question of appropriately specifying a far-field boundary condition explicitly. Furthermore, the Finite Difference method, while simple to devise and implement is not well-suited to the complex geometries of general layered media.

An attractive alternative is *surface* integral methods [3,55] (e.g. Boundary Integral Methods—BIM—or Boundary Element Methods—BEM) which only require a discretization of the layer *interfaces* (rather than the whole structure) and which, due to the choice of the Green's function, enforce the far-field boundary condition exactly. These methods can deliver high-accuracy simulations with greatly reduced operation counts, however, such formulations typically require not only the

* Corresponding author.

http://dx.doi.org/10.1016/j.jcp.2014.04.038
0021-9991/

surface trace of the field (the displacement), but also the surface trace of the *normal derivative* of the field (the traction) in order to close the set of coupled boundary conditions. "Dirichlet–Neumann Operators" (DNOs), and their generalizations, perform the operation of mapping the Dirichlet trace to its unique Neumann trace and thus it is clear that these DNOs play a central role in surface formulations. Before proceeding, we point out that DNOs have been studied in many contexts and are alternatively known as "Dirichlet-to-Neumann Maps" [16,26,30] and "Steklov–Poincaré Operators" [12].

For many problems, the layer interface shapes are moderate deviations from an exactly solvable flat-layer (infinitesimal) configuration, in which case a perturbative approach is natural. In particular, there are many low-order theories for scattering problems going back to the classical work of Rayleigh [51] and Rice [52]. In the general case we refer the interested reader to [10,11,15,18,21,23,24,27,28,33,34,42,53,57,58], while specifically to elasticity we suggest [17,22,54,59,60]. Boundary Perturbation Methods (BPMs) are built upon this philosophy, and have been shown to be a rapid, accurate, and robust class of numerical procedures for this problem (see [44] for a complete discussion and a list of references). BPMs built upon Operator Expansions [34–37,40,41], Field Expansions [4–8], and Transformed Field Expansions [45–49] have proven to be highly successful within their domains of applicability (which are *not* restricted by the *size* of the perturbation [47]), and we follow the Operator Expansions (OE) philosophy in this contribution (though other BPM could be easily imagined based upon our work here). While the developments in this contribution follow these to a certain degree, a fundamental complication of the equations of linear elastodynamics is their three-dimensional nature, not only of the independent variable, but also the unknown field. One well-known consequence of this property is that within a homogeneous medium there are *two* (body) propagation velocities, those of the primary (P-) and secondary (S-) waves. As we shall see, this plays a crucial role in our developments and distinguishes it *significantly* from the previous work.

Our approach is a Fourier/Taylor method which expands the quasiperiodic scattered field in a (generalized) Fourier series in the spatial variable, and the field in powers of the interface deformation which we characterize by a single quantity, ε, which we view as an (not necessarily small [47]) amplitude/slope. In the previous work it has been shown that the scattered fields depend *analytically* upon the parameter ε with the radius of convergence dependent on the smoothness of the interface perturbation (as rough as Lipschitz [13,25,47]). For smooth deformations the field will be *jointly* analytic with respect to both spatial and perturbation variables which results in a numerical scheme which converges exponentially as the numerical parameters are refined.

The organization of the paper is as follows: In Section 2 we recall the well-known governing equations, specialize to an elastic half-space in Section 2.1, and specify the notion of outgoing solutions in Section 2.2. In Section 3.1 we recall the classical solution in the case of a layered media with infinitesimal (vanishingly small) interfaces, and then use this to provide a formula for the Displacement-Traction Operator (DTO) in this simple case. In Section 3.2 we devise an algorithm for approximating the DTO in the important case of non-trivial geometries. Finally, in Section 4 we present numerical results which demonstrate the stability and high accuracy which our numerical algorithm can deliver.

2. Governing equations

We refer the interested reader to the very clear description in Chapter 5 of Billingham and King [2] for the governing equations of the propagation of linear waves in a solid (see also the classical text by Achenbach [1]). To summarize these developments, we recall that for small (total) displacements

$$\underline{u}^t = \underline{u}^t(x,t), \quad x \in \mathbf{R}^3,$$

of an elastic body, the governing equations are Navier's equations

$$\rho \partial_t^2 \underline{u}_i^t = \partial_j \sigma_{ij}\big(\underline{u}^t\big),$$

where ρ is the undisturbed density of the elastic solid and σ_{ij} is the symmetric stress tensor expressing the constitutive relation

$$\sigma_{ij} = \lambda e_{kk}\delta_{ij} + 2\mu e_{ij}.$$

In these, λ and μ are the Lamé constants, and δ_{ij} is the identity tensor. Substituting in the strain tensor [1], $e_{ij} = (1/2)\{\partial_j \underline{u}_i^t + \partial_i \underline{u}_j^t\}$, we arrive at (the vector form of) Navier's equation

$$\rho \partial_t^2 \underline{u}^t = (\lambda+\mu)\nabla \operatorname{div}\big[\underline{u}^t\big] + \mu \Delta \underline{u}^t.$$

If we seek time-harmonic solutions $\underline{u}^t(x,t) = \exp(-i\omega t)u^t(x)$, Navier's equation becomes

$$\mu \Delta u^t + (\lambda+\mu)\nabla \operatorname{div}\big[u^t\big] + \omega^2 \rho u^t = 0. \tag{2.1}$$

Appealing to the Helmholtz decomposition [1,2]

$$u^t = \nabla \phi^t + \operatorname{curl}\big[\psi^t\big], \qquad \operatorname{div}\big[\psi^t\big] = 0,$$

where ϕ^t is the scalar potential and ψ^t is the vector potential, (2.1) becomes

$$\nabla\big[(\lambda+2\mu)\Delta\phi^t+\omega^2\rho\phi^t\big]+\operatorname{curl}\big[\mu\Delta\psi^t+\omega^2\rho\psi^t\big]=0.$$

We can satisfy this equation by enforcing two Helmholtz equations (one scalar and one vector)

$$\Delta\phi^t+\big(\omega/c^{(1)}\big)^2\phi^t=0,\qquad \Delta\psi^t+\big(\omega/c^{(2)}\big)^2\psi^t=0,\qquad \operatorname{div}\big[\psi^t\big]=0, \tag{2.2}$$

where $c^{(1)}:=\sqrt{(\lambda+2\mu)/\rho}$ and $c^{(2)}:=\sqrt{\mu/\rho}$ are the primary wave (P-wave) and secondary wave (S-wave) velocities, respectively.

2.1. Plane harmonic waves in elastic half-space

The problem we wish to study is the reflection of an incident plane wave in an elastic half-space adjoining a medium which does not transmit mechanical waves. In particular, we focus upon incident plane-waves

$$u^i=Ae^{\mathrm{i}(\alpha\cdot\tilde{x}-\gamma x_3)},\quad A\in\mathbf{R}^3,\ \alpha=(\alpha_1,\alpha_2)^T,\ \tilde{x}=(x_1,x_2)^T,$$

impinging from above upon a periodic interface

$$x_3=g(\tilde{x}),\qquad g(\tilde{x}+\tilde{d})=g(\tilde{x}),\qquad \tilde{d}=(d_1,d_2)^T,$$

where the solid occupies the domain $x_3>g(\tilde{x})$. This incident radiation will satisfy (2.1) provided that either

$$\gamma^2=\big(\omega/c^{(1)}\big)^2-|\alpha|^2,\quad \text{and } A \text{ parallel to } (\alpha,-\gamma)^T,$$

or

$$\gamma^2=\big(\omega/c^{(2)}\big)^2-|\alpha|^2,\quad \text{and } A \text{ orthogonal to } (\alpha,-\gamma)^T,$$

while α can be freely chosen. Such an incident plane-wave will generate scattered surface displacements, u, satisfying the boundary condition

$$u\big(\tilde{x},g(\tilde{x})\big)=\xi(\tilde{x}):=-u^i\big(\tilde{x},g(\tilde{x})\big).$$

Due to the linear character of the problem the scattered displacement also satisfies the Navier equation, cf. (2.1),

$$\mu\Delta u+(\lambda+\mu)\nabla\operatorname{div}[u]+\omega^2\rho u=0, \tag{2.3}$$

and, upon appealing to the Helmholtz decomposition, the Helmholtz equations, cf. (2.2),

$$\Delta\phi+\big(\omega/c^{(1)}\big)^2\phi=0,\qquad \Delta\psi+\big(\omega/c^{(2)}\big)^2\psi=0,\qquad \operatorname{div}[\psi]=0. \tag{2.4}$$

This problem is known to have a unique, α-quasiperiodic,

$$u(\tilde{x}+\tilde{d},x_3)=e^{\mathrm{i}\alpha\cdot\tilde{d}}u(\tilde{x},x_3),$$

solution which is outgoing [1].

2.2. Outgoing solutions

To make the notion of outgoing solutions more precise, for $x_3>|g|_{L^\infty}$, the exact solutions (given by the Rayleigh expansions) for the Helmholtz equations, (2.4), are

$$\phi(x)=\sum_{|p|=-\infty}^{\infty}\hat{\phi}(p)e^{\mathrm{i}(\alpha(p)\cdot\tilde{x}+\gamma^{(1)}(p)x_3)},\qquad \psi(x)=\sum_{|p|=-\infty}^{\infty}\hat{\psi}(p)e^{\mathrm{i}(\alpha(p)\cdot\tilde{x}+\gamma^{(2)}(p)x_3)}, \tag{2.5}$$

where $\psi(x)$ must be divergence-free. In these formulas $p=(p_1,p_2)^T\in\mathbf{Z}^2$ (so that the summation notation above is shorthand for the double sum over all $p\in\mathbf{Z}^2$) and

$$\alpha(p)=\alpha+2\pi\begin{pmatrix}p_1/d_1\\ p_2/d_2\end{pmatrix}$$

$$\gamma^{(j)}(p)=\begin{cases}\sqrt{(\omega/c^{(j)})^2-|\alpha(p)|^2}, & |\alpha(p)|^2<(\omega/c^{(j)})^2\\ \mathrm{i}\sqrt{|\alpha(p)|^2-(\omega/c^{(j)})^2}, & |\alpha(p)|^2>(\omega/c^{(j)})^2\end{cases},\quad j=1,2.$$

The outgoing wave condition is reflected in the choice of the positive signs before $\gamma^{(j)}(p)$ in the expressions for ϕ and ψ in (2.5).

With the definition of the wavevector

$$\kappa^{(j)}(p) := \begin{pmatrix} \alpha(p) \\ \gamma^{(j)}(p) \end{pmatrix},$$

we can write

$$\phi(x) = \sum_{|p|=-\infty}^{\infty} \hat{\phi}(p) e^{\mathrm{i}\kappa^{(1)}(p)\cdot x}, \qquad \psi(x) = \sum_{|p|=-\infty}^{\infty} \hat{\psi}(p) e^{\mathrm{i}\kappa^{(2)}(p)\cdot x}, \quad \mathrm{i}\kappa^{(2)}(p)\cdot\hat{\psi}(p) = 0.$$

We can now express the scattered elastic wave field as

$$u(x) = \nabla\phi + \mathrm{curl}[\psi] = \sum_{|p|=-\infty}^{\infty} \left(\mathrm{i}\kappa^{(1)}(p)\right)\hat{\phi}(p) e^{\mathrm{i}\kappa^{(1)}(p)\cdot x} + \sum_{|p|=-\infty}^{\infty} \left\{\left(\mathrm{i}\kappa^{(2)}(p)\right) \times \hat{\psi}(p)\right\} e^{\mathrm{i}\kappa^{(2)}(p)\cdot x},$$
$$\left(\mathrm{i}\kappa^{(2)}(p)\right)\cdot\hat{\psi}(p) = 0. \tag{2.6}$$

Remark 2.1. In this expression the *scalar* coefficient $\hat{\phi}(p)$ delivers the P-waves, while the *vector* quantity $\{(\mathrm{i}\kappa^{(2)}(p)) \times \hat{\psi}(p)\}$ gives the S-waves. Due to the orthogonality constraint

$$\left(\mathrm{i}\kappa^{(2)}(p)\right)\cdot\hat{\psi}(p) = 0,$$

the latter lies in a two-dimensional space which can be spanned by a vector in the vertical plane (the SV-waves) and one in the horizontal plane (the SH-waves). Therefore (2.6) captures all of the body waves which propagate in a homogeneous, isotropic solid.

3. The displacement-traction operator

The fundamental object of our study is a generalized Dirichlet–Neumann Operator (DNO), namely the Displacement-Traction Operator (DTO), which we define here.

Definition 3.1. Consider the time-harmonic Navier's equations, (2.3),

$$\mu\Delta u + (\lambda+\mu)\nabla\,\mathrm{div}[u] + \omega^2\rho u = 0, \quad x_3 > g(\tilde{x}),$$

supplemented with displacement (Dirichlet) data

$$u\left(\tilde{x}, g(\tilde{x})\right) = \xi(\tilde{x}). \tag{3.1}$$

The unique, α-quasiperiodic, outgoing solution delivers the surface traction (normal stress; Neumann) data

$$\nu_i(\tilde{x}) = \sigma_{ij}(u)|_{x_3=g} N_j,$$

with exterior normal

$$N = (\partial_1 g, \partial_2 g, -1)^T,$$

and the Displacement-Traction Operator (DTO), G, is defined as the operation of computing ν given ξ,

$$G(g) : \xi \to \nu.$$

Remark 3.2. In light of the relation

$$\sigma_{ij} = \lambda e_{kk}\delta_{ij} + 2\mu e_{ij},$$

we introduce the notation $G = L + M$ where

$$L := \lambda e_{kk}\delta_{ij}N_j|_{x_3=g} = \lambda e_{kk}N_i|_{x_3=g}, \qquad M := 2\mu e_{ij}N_j|_{x_3=g}. \tag{3.2}$$

Clearly, the DTO depends *linearly* upon the Dirichlet data ξ, while the dependence on g is *nonlinear*. However, this dependence is *analytic* and we use this fact to great effect to produce a robust high-order numerical algorithm.

3.1. Infinitesimal deformations

Before coming to this, we begin with the (relatively) simple case of the DTO in the case of an infinitesimal (non-zero but vanishingly small) interface that we model by $g \equiv 0$ with normal $N_i = -\delta_{i3}$. While this is not the focus of our study, it is the "base case" which allows us to address non-zero deformations.

The first step is to find the unique solution to Navier's equation with displacement boundary condition, (3.1). From (2.6) we have

$$\sum_{|p|=-\infty}^{\infty} \hat{\xi}(p) e^{\mathrm{i}\alpha(p)\cdot\tilde{x}} = \xi(\tilde{x}) = u(\tilde{x},0) = \sum_{|p|=-\infty}^{\infty} \left[\left(\mathrm{i}\kappa^{(1)}(p)\right)\hat{\phi}(p) + \left\{\left(\mathrm{i}\kappa^{(2)}(p)\right) \times \hat{\psi}(p)\right\}\right] e^{\mathrm{i}\alpha(p)\cdot\tilde{x}},$$

subject to $(\mathrm{i}\kappa^{(2)}(p)) \cdot \hat{\psi}(p) = 0$. The solution is found by solving the *linear* system of equations

$$\begin{pmatrix} \mathrm{i}\kappa^{(2)}(p)\times & \mathrm{i}\kappa^{(1)}(p) \\ \mathrm{i}\kappa^{(2)}(p)^T & 0 \end{pmatrix} \begin{pmatrix} \hat{\psi}(p) \\ \hat{\phi}(p) \end{pmatrix} = \begin{pmatrix} \hat{\xi}(p) \\ 0 \end{pmatrix},$$

which, for each p, is four equations in four unknowns. We denote the solution map by

$$\hat{\psi}(p) = \mathcal{L}_\psi\left[\hat{\xi}(p)\right], \qquad \hat{\phi}(p) = \mathcal{L}_\phi\left[\hat{\xi}(p)\right].$$

Regarding the operator $L = L(0)$, from (2.6) we have

$$e_{kk}(x) = \partial_k u_k(x) = \sum_{|p|=-\infty}^{\infty} \left(\mathrm{i}\kappa^{(1)}(p)\right) \cdot \left(\mathrm{i}\kappa^{(1)}(p)\right)\hat{\phi}(p) e^{\mathrm{i}\kappa^{(1)}(p)\cdot x} = \sum_{|p|=-\infty}^{\infty} -\left|\kappa^{(1)}(p)\right|^2 \hat{\phi}(p) e^{\mathrm{i}\kappa^{(1)}(p)\cdot x},$$

so that

$$L(0)[\xi] = \sum_{|p|=-\infty}^{\infty} \lambda \left|\kappa^{(1)}(p)\right|^2 \mathcal{L}_\phi\left[\hat{\xi}(p)\right] e^{\mathrm{i}\alpha(p)\cdot\tilde{x}}\delta_{i3}. \tag{3.3}$$

For $M = M(0)$ we compute

$$\partial_j u_i(x) = \sum_{|p|=-\infty}^{\infty} \left(\mathrm{i}\kappa_j^{(1)}(p)\right)\left(\mathrm{i}\kappa_i^{(1)}(p)\right)\hat{\phi}(p) e^{\mathrm{i}\kappa^{(1)}(p)\cdot x} + \sum_{|p|=-\infty}^{\infty} \left(\mathrm{i}\kappa_j^{(2)}(p)\right)\left\{\left(\mathrm{i}\kappa^{(2)}(p)\right) \times \hat{\psi}(p)\right\}_i e^{\mathrm{i}\kappa^{(2)}(p)\cdot x},$$

again subject to $(\mathrm{i}\kappa^{(2)}(p)) \cdot \hat{\psi}(p) = 0$. So

$$\begin{aligned} 2e_{ij} = \partial_j u_i + \partial_i u_j = &\sum_{|p|=-\infty}^{\infty} 2\left(\mathrm{i}\kappa_j^{(1)}(p)\right)\left(\mathrm{i}\kappa_i^{(1)}(p)\right)\hat{\phi}(p) e^{\mathrm{i}\kappa^{(1)}(p)\cdot x} \\ &+ \sum_{|p|=-\infty}^{\infty} \left[\left(\mathrm{i}\kappa_j^{(2)}(p)\right)\left\{\left(\mathrm{i}\kappa^{(2)}(p)\right) \times \hat{\psi}(p)\right\}_i + \left(\mathrm{i}\kappa_i^{(2)}(p)\right)\left\{\left(\mathrm{i}\kappa^{(2)}(p)\right) \times \hat{\psi}(p)\right\}_j\right] e^{\mathrm{i}\kappa^{(2)}(p)\cdot x}, \end{aligned}$$

and

$$\begin{aligned} M(0)[\xi] &= 2\mu e_{ij} N_{j3}|_{x_3=0} = -2\mu e_{ij}\delta_{j3}|_{x_3=0} \\ &= \mu \sum_{|p|=-\infty}^{\infty} \left[2\kappa_j^{(1)}(p)\kappa_i^{(1)}(p)\hat{\phi}(p) + \kappa_j^{(2)}(p)\left\{\kappa^{(2)}(p) \times \hat{\psi}(p)\right\}_i + \kappa_i^{(2)}(p)\left\{\kappa^{(2)}(p) \times \hat{\psi}(p)\right\}_j\right] e^{\mathrm{i}\alpha(p)\cdot\tilde{x}}\delta_{j3} \\ &= \mu \sum_{|p|=-\infty}^{\infty} \left[2\kappa_j^{(1)}(p)\kappa_i^{(1)}(p)\mathcal{L}_\phi\left[\hat{\xi}(p)\right]\right. \\ &\quad \left. + \kappa_j^{(2)}(p)\left\{\kappa^{(2)}(p) \times \mathcal{L}_\psi\left[\hat{\xi}(p)\right]\right\}_i + \kappa_i^{(2)}(p)\left\{\kappa^{(2)}(p) \times \mathcal{L}_\psi\left[\hat{\xi}(p)\right]\right\}_j\right] e^{\mathrm{i}\alpha(p)\cdot\tilde{x}}\delta_{j3}. \end{aligned} \tag{3.4}$$

3.2. General deformations

We now move to the general setting of DTOs connected to non-trivial geometries with interface shaped by the graph of the function $x_3 = g(\tilde{x})$. Of course this is generally quite a difficult problem and the key to our approach is to consider deformations of the form

$$g(\tilde{x}) = \varepsilon f(\tilde{x}),$$

which gives rise to expansions

$$u = u(x;\varepsilon) = \sum_{n=0}^{\infty} u^{(n)}(x)\varepsilon^n, \qquad L = L(\varepsilon) = \sum_{n=0}^{\infty} L^{(n)}\varepsilon^n, \qquad M = M(\varepsilon) = \sum_{n=0}^{\infty} M^{(n)}\varepsilon^n,$$

that can be shown to be strongly convergent [25,45,47]. We now outline the Method of Operator Expansions (OE) [14,34,35,48] for simulating DTO in this setting of linear elastodynamics.

To begin our development consider the following α-quasiperiodic, outgoing solution of the time-harmonic Navier's equation

$$u(x;p) = \big(\mathrm{i}\kappa^{(1)}(p)\big)\hat{\phi}(p)e^{\mathrm{i}\kappa^{(1)}(p)\cdot x} + \big\{\big(\mathrm{i}\kappa^{(2)}(p)\big)\times\hat{\psi}(p)\big\}e^{\mathrm{i}\kappa^{(2)}(p)\cdot x}, \tag{3.5}$$

subject to $(\mathrm{i}\kappa^{(2)}(p))\cdot\hat{\psi}(p) = 0$. We note that, in terms of these, (2.6) can be written as

$$u(x) = \sum_{|p|=-\infty}^{\infty} u(x;p), \qquad \big(\mathrm{i}\kappa^{(2)}(p)\big)\cdot\hat{\psi}(p) = 0.$$

We now define the *surface* quantities

$$U(\tilde{x};g,p) := u\big(\tilde{x},g(\tilde{x});p\big) \tag{3.6a}$$

$$K(\tilde{x};g,p) := \partial_k u_k\big(\tilde{x},g(\tilde{x});p\big) \tag{3.6b}$$

$$E_{ij}(\tilde{x};g,p) := \big\{\partial_j u_i\big(\tilde{x},g(\tilde{x});p\big) + \partial_i u_j\big(\tilde{x},g(\tilde{x});p\big)\big\}, \tag{3.6c}$$

and observe that, expressing $g = \varepsilon f$, these are analytic in ε so that

$$\{U,K,E_{ij}\}(\tilde{x};\varepsilon f,p) = \sum_{n=0}^{\infty}\big\{U^{(n)}(\tilde{x};p),K^{(n)}(\tilde{x};p),E_{ij}^{(n)}(\tilde{x};p)\big\}\varepsilon^n.$$

We will derive forms for the $\{U^{(n)},K^{(n)},E_{ij}^{(n)}\}$ in Appendix A.

Turning to the operator L, from (3.2) we can write

$$L(\varepsilon f)\big[U(\tilde{x};\varepsilon f,p)\big] = \lambda K(\tilde{x};\varepsilon f,p)N_i(\varepsilon f),$$

and expand

$$\left(\sum_{n=0}^{\infty}\varepsilon^n L^{(n)}(f)\right)\left[\sum_{m=0}^{\infty}U^{(m)}(\tilde{x};f,p)\varepsilon^m\right] = \lambda(\varepsilon\partial_1 f)\sum_{n=0}^{\infty}K^{(n)}(\tilde{x};f,p)\varepsilon^n\delta_{i1} + \lambda(\varepsilon\partial_2 f)\sum_{n=0}^{\infty}K^{(n)}(\tilde{x};f,p)\varepsilon^n\delta_{i2} - \lambda\sum_{n=0}^{\infty}K^{(n)}(\tilde{x};f,p)\varepsilon^n\delta_{i3}.$$

Equating at order zero we find

$$L^{(0)}\big[U^{(0)}\big] = -\lambda K^{(0)}\delta_{i3},$$

where

$$U^{(0)} = u(\tilde{x},0;p) = \big(\mathrm{i}\kappa^{(1)}(p)\big)\hat{\phi}(p)e^{\mathrm{i}\alpha(p)\cdot\tilde{x}} + \big\{\big(\mathrm{i}\kappa^{(2)}(p)\big)\times\hat{\psi}(p)\big\}e^{\mathrm{i}\alpha(p)\cdot\tilde{x}} = \hat{\xi}(p)e^{\mathrm{i}\alpha(p)\cdot\tilde{x}}$$

$$K^{(0)} = -\big|\kappa^{(1)}(p)\big|^2\hat{\phi}(p)e^{\mathrm{i}\alpha(p)\cdot\tilde{x}} = -\big|\kappa^{(1)}(p)\big|^2\mathcal{L}_\phi\big[\hat{\xi}(p)\big]e^{\mathrm{i}\alpha(p)\cdot\tilde{x}},$$

so that we recover (3.3)

$$L(0)\big[\hat{\xi}(p)e^{\mathrm{i}\alpha(p)\cdot\tilde{x}}\big] = \lambda\big|\kappa^{(1)}(p)\big|^2\mathcal{L}_\phi\big[\hat{\xi}(p)\big]e^{\mathrm{i}\alpha(p)\cdot\tilde{x}}\delta_{i3}.$$

At order $n>0$ we find

$$L^{(n)}(f)\big[\hat{\xi}(p)e^{\mathrm{i}\alpha(p)\cdot\tilde{x}}\big] = L^{(n)}(f)\big[U^{(0)}\big] = -\lambda K^{(n)}(f)\delta_{i3} + \lambda(\partial_1 f)K^{(n-1)}(f)\delta_{i1} + \lambda(\partial_2 f)K^{(n-1)}(f)\delta_{i2} - \sum_{m=0}^{n-1}L^{(m)}(f)\big[U^{(n-m)}\big]. \tag{3.7}$$

In an exactly analogous fashion we can show that

$$M^{(0)}\big[\hat{\xi}(p)e^{\mathrm{i}\alpha(p)\cdot\tilde{x}}\big] = M^{(0)}\big[U^{(0)}\big] = \mu E^{(0)}_{ij}\delta_{j3}$$
$$= \mu\big[2\kappa^{(1)}_j(p)\kappa^{(1)}_i(p)\mathcal{L}_\phi\big[\hat{\xi}(p)\big]$$
$$+\kappa^{(2)}_j(p)\big\{\kappa^{(2)}(p)\times\mathcal{L}_\psi\big[\hat{\xi}(p)\big]\big\}_i + \kappa^{(2)}_i(p)\big\{\kappa^{(2)}(p)\times\mathcal{L}_\psi\big[\hat{\xi}(p)\big]\big\}_j\big]\delta_{j3},$$

which recovers (3.4), and

$$M^{(n)}(f)\big[U^{(0)}\big] = -\mu E^{(n)}_{i3}(f) + \mu(\partial_1 f)E^{(n-1)}_{i1}(f) + \mu(\partial_2 f)E^{(n-1)}_{i2}(f) - \sum_{m=0}^{n-1} M^{(m)}(f)\big[U^{(n-m)}\big]. \tag{3.8}$$

Of course the key to all of these developments is the derivation of useful forms for the $\{U^{(n)}, K^{(n)}, E^{(n)}_{ij}\}$ which we describe in Appendix A.

4. Numerical results

We now provide detailed results of numerical simulations of scattering quantities compared with *exact* solutions. We show that our numerical method is efficient and accurate, and applicable to quite general configurations.

4.1. Exact solutions

Naturally, for a problem as complicated as what we consider here (that of non-trivial interfaces), there are no known exact solutions. Thus, to perform a convergence study for our algorithm we utilize the following principle: When implementing a solver for the homogeneous problem:

$$\mathcal{L}u = 0 \quad \text{in } \Omega$$
$$\mathcal{B}u = 0 \quad \text{at } \partial\Omega,$$

it is usually no more difficult to construct a method for the corresponding inhomogeneous problem:

$$\mathcal{L}u = \mathcal{R} \quad \text{in } \Omega$$
$$\mathcal{B}u = \mathcal{Q} \quad \text{at } \partial\Omega.$$

For any function w, we can compute

$$\mathcal{R}_w := \mathcal{L}w, \qquad \mathcal{Q}_w := \mathcal{B}w,$$

and realize an *exact* solution to the problem

$$\mathcal{L}u = \mathcal{R}_w \quad \text{in } \Omega$$
$$\mathcal{B}u = \mathcal{Q}_w \quad \text{at } \partial\Omega,$$

namely $u = w$. Thus, we have a means to test the inhomogeneous solver in this (special) case. However, it is the most helpful to consider w which have the same "behavior" as solutions u of the inhomogeneous problem and here we specify w such that $\mathcal{R}_w \equiv 0$. These exact solutions correspond to plane-wave *reflection* rather than *incidence*.

More specifically, we consider the functions, cf. (3.5),

$$u(x;p) = \big(\mathrm{i}\kappa^{(1)}(p)\big)\hat{\Phi}(p)e^{\mathrm{i}\kappa^{(1)}(p)\cdot x} + \big\{\big(\mathrm{i}\kappa^{(2)}(p)\big)\times\hat{\Psi}(p)\big\}e^{\mathrm{i}\kappa^{(2)}(p)\cdot x}, \tag{4.1}$$

which, for any choice of integer p, real $\hat{\Phi}(p)$, and real three-vector $\hat{\Psi}(p)$ such that $\mathrm{i}\kappa^{(2)}(p)\cdot\hat{\Psi}(p) = 0$, satisfy Navier's equations (2.3) and is outgoing so that $\mathcal{R}_w \equiv 0$. However, the boundary conditions satisfied by these functions are *not* those satisfied by an incident plane wave. With the construction of the $\mathcal{Q}_w$ in mind we compute the surface data

$$\xi(\tilde{x};p) = u\big(\tilde{x}, g(\tilde{x});p\big) = \big[\big(\mathrm{i}\kappa^{(1)}(p)\big)\hat{\Phi}(p)e^{\mathrm{i}\gamma^{(1)}(p)g(\tilde{x})} + \big\{\big(\mathrm{i}\kappa^{(2)}(p)\big)\times\hat{\Psi}(p)\big\}e^{\mathrm{i}\gamma^{(2)}(p)g(\tilde{x})}\big]e^{i\alpha(p)\cdot\tilde{x}}.$$

We now have a family of exact solutions against which to test our numerical algorithm for *any* choice of deformation $g(\tilde{x})$.

4.2. Numerical implementation

The description of our numerical scheme is not complicated which, in our view, is a distinct advantage of our method. Our Boundary Perturbation approach posits, for instance, an expansion of the traction in the form

$$v(\tilde{x};\varepsilon)=\sum_{n=0}^{\infty} v^{(n)}(\tilde{x})\varepsilon^n$$

and we seek as an approximation, the truncation of this Taylor series after N terms

$$v^N(\tilde{x};\varepsilon):=\sum_{n=0}^{N} v^{(n)}(\tilde{x})\varepsilon^n.$$

Without approximation we can recover the $v^{(n)}$ from the formulas (3.3) and (3.4) at order zero, and (3.7) and (3.8) for $n>0$. However, the functions which appear in these formulas generally involve Fourier series with an infinite number of non-zero coefficients. Thus, we make a spectral approximation to each of the $v^{(n)}(\tilde{x})$ by

$$v^{n,N_x}(\tilde{x}):=\sum_{|p|=-N_x/2}^{N_x/2-1}\hat{v}^{(n)}(p)e^{i\alpha(p)\cdot\tilde{x}}. \tag{4.2}$$

Products appearing in (3.3), (3.4), (3.7), and (3.8) are computed by fast convolutions via the Fast Fourier Transform (FFT) algorithm [19] and our final Fourier/Taylor approximation is

$$v^{N,N_x}(\tilde{x};\varepsilon):=\sum_{n=0}^{N}\sum_{|p|=-N_x/2}^{N_x/2-1}\hat{v}^{(n)}(p)e^{i\alpha(p)\cdot\tilde{x}}\varepsilon^n. \tag{4.3}$$

Before leaving our discussion of the numerical scheme, we address one (initially) subtle, but crucially important consideration which can be effectively demonstrated in the formula for $L^{(n)}$, (3.7). Careful inspection of this formula reveals its *recursive* nature: In order to compute $L^{(n)}[\psi]$ one needs to evaluate $L^{(n-1)}$ applied to the function $U^{(1)}$ which, in turn requires the evaluation of $L^{(n-2)}$ applied to $U^{(1)}$, etc. Clearly, the complexity of this formula is $\mathcal{O}(N_x\log(N_x)n!)$.

In the previous work we have shown [43,48] how adjointness properties of these operators can be used to reduce this to $\mathcal{O}(N_x\log(N_x)n^2)$, however, we have been unable (thus far) to reproduce this success in this setting. However, there is an alternative which avoids the prohibitive factorial cost of a direct implementation of (3.7). For this we *store* at every perturbation order the action of $L^{(n)}$ as a matrix acting on the basis functions $\exp(i\alpha(p)\cdot\tilde{x})$ evaluated at the equally spaced gridpoints $\tilde{x}_l$. While this is far from optimal (at every perturbation order one must evaluate at every wavenumber p which we represent, of order $\mathcal{O}(N_x^2n^2)$), it certainly makes our algorithm feasible.

4.3. Error measurement

With these numerical approximations we can make error measurements versus the exact solutions (4.1). We choose to measure the defect in the traction which is quite difficult due to the fact that this data is posed on the very surfaces around which we perturb. For the results described in Section 4.4 we measure the relative supremum norm,

$$\text{Error}_{\text{rel}}(N,N_x)=\frac{|v-v^{N,N_x}|_{L^\infty}}{|v|_{L^\infty}}. \tag{4.4}$$

4.4. Numerical tests

We now consider a $(2\pi)\times(2\pi)$ periodic interface bounding a three-dimensional solid. We follow the lead of [38,46] and select the following interface shapes: The cosine

$$f_s(x_1,x_2)=\cos(x_1+x_2), \tag{4.5a}$$

the analytic profile,

$$f_a(x_1,x_2)=W(x_1)W(x_2), \tag{4.5b}$$

where

$$W(z)=\frac{B^2\cos(z)-B}{B^2+1-2B\cos(z)},\quad B=(2\rho)^{-1/(R-1)},\ \rho=10^{-16},\ R=10,$$

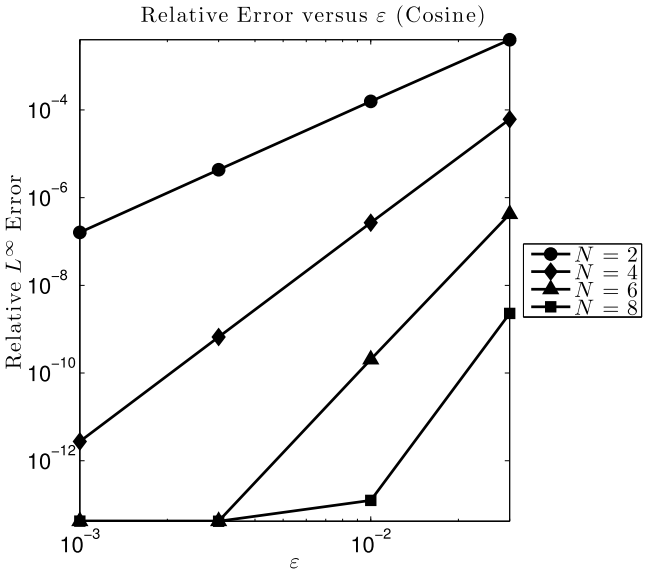

Fig. 1. Plot of relative L^∞ error versus perturbation order N for the cosine profile, (4.5a) ($\varepsilon = 10^{-3}, 3\times10^{-3}, 10^{-2}, 3\times10^{-2}$).

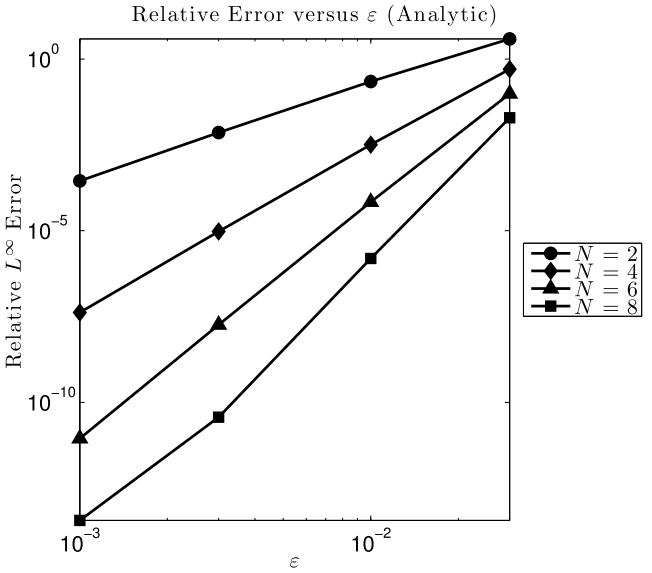

Fig. 2. Plot of relative L^∞ error versus perturbation order N for the analytic profile, (4.5b) ($\varepsilon = 10^{-3}, 3\times10^{-3}, 10^{-2}, 3\times10^{-2}$).

the "rough" (C^2 but not C^3) profile

$$f_r(x_1,x_2) = \left(\frac{2}{9}\times 10^{-3}\right)\left\{x_1^2(2\pi - x_1)^2 x_2^2(2\pi - x_2)^2 - \frac{64\pi^8}{225}\right\}, \tag{4.5c}$$

and the Lipschitz boundary

$$f_L(x_1,x_2) = \frac{1}{3} + \begin{cases} -1 + (2/\pi)x_1, & x_1 \le x_2 \le 2\pi - x_1 \\ 3 - (2/\pi)x_2, & x_2 > x_1,\ x_2 > 2\pi - x_1 \\ 3 - (2/\pi)x_1, & 2\pi - x_1 < x_2 < x_1 \\ -1 + (2/\pi)x_2, & x_2 < x_1,\ x_2 < 2\pi - x_1. \end{cases} \tag{4.5d}$$

All four profiles have zero mean, approximate amplitude 2, and maximum slope of roughly 1. To clarify the choice f_a we point out [38] that the Fourier coefficients of W are

$$\hat{W}_p = \begin{cases} \frac{1}{2}(2\rho)^{(|p|-1)/(R-1)} & p \neq 0 \\ 0 & p = 0 \end{cases}$$

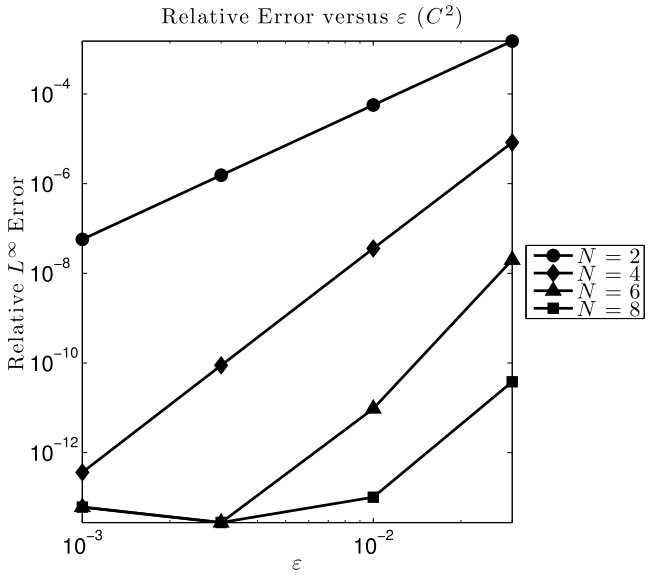

Fig. 3. Plot of relative L^∞ error versus perturbation order N for the C^2 profile, (4.5c) ($\varepsilon = 10^{-3}$, 3×10^{-3}, 10^{-2}, 3×10^{-2}).

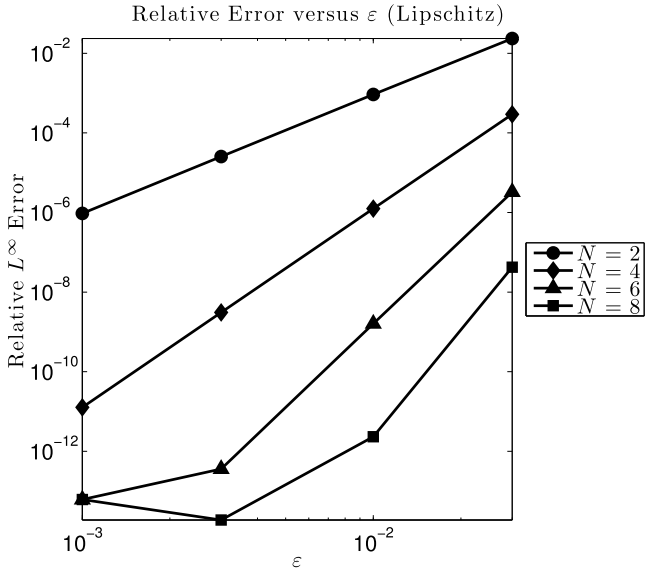

Fig. 4. Plot of relative L^∞ error versus perturbation order N for the Lipschitz profile, (4.5d) ($\varepsilon = 10^{-3}$, 3×10^{-3}, 10^{-2}, 3×10^{-2}).

so that the profile has mean zero, $\hat{W}_1 = \hat{W}_{-1} = 1/2$ like the cosine, the coefficients decay exponentially fast (giving analyticity of the profile), and the R-th coefficient has value ρ.

In Figs. 1, 2, 3, and 4 we display results of our numerical simulations for the cosine, (4.5a), analytic, (4.5b), C^2, (4.5c), and Lipschitz, (4.5d), profiles respectively, for values of $\varepsilon = 10^{-3}, 3 \times 10^{-3}, 10^{-2}, 3 \times 10^{-2}$. For physical parameters we picked values meant to be representative of steel [2]

$$\rho = 7800, \qquad \lambda = 8.6 \times 10^{10}, \qquad \mu = 7.9 \times 10^{10},$$

so that $c^{(1)} \approx 5600$ and $c^{(2)} \approx 3180$, and the academic value $\omega = 8000$ under normal illumination so that

$$\left|\kappa^{(1)}\right| = \omega / c^{(1)} \approx 1.429, \qquad \left|\kappa^{(2)}\right| = \omega / c^{(2)} \approx 2.516.$$

For all four simulations we have chosen numerical parameters $N_{x_1} = N_{x_2} = 8$ and perturbation orders $N = 0, \ldots, 10$. In all four cases we see the rapid and stable convergence which our algorithm delivers in agreement with the spectral properties our Fourier/Taylor approach should satisfy.

Acknowledgements

D.P.N. gratefully acknowledges support from the National Science Foundation through grant No. DMS-1115333, and the Department of Energy under Award No. DE-SC0001549.

Appendix A. Recursive formulas for the $U^{(n)}$, $K^{(n)}$, and $E_{ij}^{(n)}$

Of crucial importance to our Operator Expansions approach outlined in Section 3.2 are forms for the $\{U^{(n)}, K^{(n)}, E_{ij}^{(n)}\}$, and in this section we briefly derive these. We begin by recalling the α-quasiperiodic outgoing solution of the time-harmonic Navier's equation, cf. (3.5),

$$u(x;p) = \big(\mathrm{i}\kappa^{(1)}(p)\big)\hat{\phi}(p)e^{\mathrm{i}\kappa^{(1)}(p)\cdot x} + \big\{\big(\mathrm{i}\kappa^{(2)}(p)\big)\times\hat{\psi}(p)\big\}e^{\mathrm{i}\kappa^{(2)}(p)\cdot x},$$

and the surface quantities, cf. (3.6),

$$\begin{aligned}
U(\tilde{x};g,p) &= u\big(\tilde{x},g(\tilde{x});p\big)\\
K(\tilde{x};g,p) &= \partial_k u_k\big(\tilde{x},g(\tilde{x});p\big)\\
E_{ij}(\tilde{x};g,p) &= \big\{\partial_j u_i\big(\tilde{x},g(\tilde{x});p\big)+\partial_i u_j\big(\tilde{x},g(\tilde{x});p\big)\big\}.
\end{aligned}$$

We begin with the $U^{(n)}$ by writing

$$U(\tilde{x};\varepsilon f,p) = \big\{\big(\mathrm{i}\kappa^{(1)}(p)\big)\hat{\phi}(p)e^{\mathrm{i}\gamma^{(1)}(p)\varepsilon f} + \big(\mathrm{i}\kappa^{(2)}(p)\big)\times\hat{\psi}(p)e^{\mathrm{i}\gamma^{(2)}(p)\varepsilon f}\big\}e^{\mathrm{i}\alpha(p)\cdot\tilde{x}}$$

so that

$$\sum_{n=0}^{\infty}U^{(n)}\varepsilon^n = \sum_{n=0}^{\infty}\varepsilon^n F_n\big\{\big(\mathrm{i}\gamma^{(1)}(p)\big)^n\big(\mathrm{i}\kappa^{(1)}(p)\big)\hat{\phi}(p)+\big(\mathrm{i}\gamma^{(2)}(p)\big)^n\big(\mathrm{i}\kappa^{(2)}(p)\big)\times\hat{\psi}(p)\big\}e^{\mathrm{i}\alpha(p)\cdot\tilde{x}},$$

where $F_n = f^n/n!$. Thus

$$\begin{aligned}
U^{(0)} &= \big\{\big(\mathrm{i}\kappa^{(1)}(p)\big)\hat{\phi}(p)+\big(\mathrm{i}\kappa^{(2)}(p)\big)\times\hat{\psi}(p)\big\}e^{\mathrm{i}\alpha(p)\cdot\tilde{x}}\\
&= \big\{\big(\mathrm{i}\kappa^{(1)}(p)\big)\mathcal{L}_\phi\big[\hat{\xi}(p)\big]+\big(\mathrm{i}\kappa^{(2)}(p)\big)\times\mathcal{L}_\psi\big[\hat{\xi}(p)\big]\big\}e^{\mathrm{i}\alpha(p)\cdot\tilde{x}}\\
&= \hat{\xi}(p)e^{\mathrm{i}\alpha(p)\cdot\tilde{x}},
\end{aligned}$$

and, for $n>0$,

$$\begin{aligned}
U^{(n)} &= F_n\big\{\big(\mathrm{i}\gamma^{(1)}(p)\big)^n\big(\mathrm{i}\kappa^{(1)}(p)\big)\hat{\phi}(p)+\big(\mathrm{i}\gamma^{(2)}(p)\big)^n\big(\mathrm{i}\kappa^{(2)}(p)\big)\times\hat{\psi}(p)\big\}e^{\mathrm{i}\alpha(p)\cdot\tilde{x}}\\
&= F_n\big\{\big(\mathrm{i}\gamma^{(1)}(p)\big)^n\big(\mathrm{i}\kappa^{(1)}(p)\big)\mathcal{L}_\phi\big[\hat{\xi}(p)\big]+\big(\mathrm{i}\gamma^{(2)}(p)\big)^n\big(\mathrm{i}\kappa^{(2)}(p)\big)\times\mathcal{L}_\psi\big[\hat{\xi}(p)\big]\big\}e^{\mathrm{i}\alpha(p)\cdot\tilde{x}}.
\end{aligned}$$

Moving to $K^{(n)}$ we write

$$K(\tilde{x};\varepsilon f,p) = -\big|\kappa^{(1)}(p)\big|^2\hat{\phi}(p)e^{\mathrm{i}\gamma^{(1)}(p)\varepsilon f}e^{\mathrm{i}\alpha(p)\cdot\tilde{x}},$$

so that

$$\sum_{n=0}^{\infty}K^{(n)}\varepsilon^n = -\sum_{n=0}^{\infty}\varepsilon^n F_n\big(\mathrm{i}\gamma^{(1)}(p)\big)^n\big|\kappa^{(1)}(p)\big|^2\hat{\phi}(p)e^{\mathrm{i}\alpha(p)\cdot\tilde{x}}.$$

Thus

$$\begin{aligned}
K^{(0)} &= -\big|\kappa^{(1)}(p)\big|^2\hat{\phi}(p)e^{\mathrm{i}\alpha(p)\cdot\tilde{x}}\\
&= -\big|\kappa^{(1)}(p)\big|^2\mathcal{L}_\phi\big[\hat{\xi}(p)\big]e^{\mathrm{i}\alpha(p)\cdot\tilde{x}},
\end{aligned}$$

and, for $n>0$,

$$\begin{aligned}
K^{(n)} &= -F_n\big(\mathrm{i}\gamma^{(1)}(p)\big)^n\big|\kappa^{(1)}(p)\big|^2\hat{\phi}(p)e^{\mathrm{i}\alpha(p)\cdot\tilde{x}}\\
&= -F_n\big(\mathrm{i}\gamma^{(1)}(p)\big)^n\big|\kappa^{(1)}(p)\big|^2\mathcal{L}_\phi\big[\hat{\xi}(p)\big]e^{\mathrm{i}\alpha(p)\cdot\tilde{x}}.
\end{aligned}$$

To close, consider $E_{ij}^{(n)}$ by writing

$$E_{ij}(\tilde{x};\varepsilon f,p)=\big\{2\big(\mathrm{i}\kappa_j^{(1)}(p)\big)\big(\mathrm{i}\kappa_i^{(1)}(p)\big)\hat{\phi}(p)e^{\mathrm{i}\gamma^{(1)}(p)\varepsilon f}+\big[\big(\mathrm{i}\kappa_j^{(2)}(p)\big)\big\{\big(\mathrm{i}\kappa^{(2)}(p)\big)\times\hat{\psi}(p)\big\}_i+\big(\mathrm{i}\kappa_i^{(2)}(p)\big)\big\{\big(\mathrm{i}\kappa^{(2)}(p)\big)\times\hat{\psi}(p)\big\}_j\big]e^{\mathrm{i}\gamma^{(2)}(p)\varepsilon f}\big\}e^{\mathrm{i}\alpha(p)\cdot\tilde{x}},$$

so that

$$\sum_{n=0}^{\infty}E_{ij}^{(n)}\varepsilon^n=\sum_{n=0}^{\infty}\varepsilon^n F_n\big\{2\big(\mathrm{i}\gamma^{(1)}(p)\big)^n\big(\mathrm{i}\kappa_j^{(1)}(p)\big)\big(\mathrm{i}\kappa_i^{(1)}(p)\big)\hat{\phi}(p)+\big(\mathrm{i}\gamma^{(2)}(p)\big)^n\big[\big(\mathrm{i}\kappa_j^{(2)}(p)\big)\big\{\big(\mathrm{i}\kappa^{(2)}(p)\big)\times\hat{\psi}(p)\big\}_i+\big(\mathrm{i}\kappa_i^{(2)}(p)\big)\big\{\big(\mathrm{i}\kappa^{(2)}(p)\big)\times\hat{\psi}(p)\big\}_j\big]\big\}e^{\mathrm{i}\alpha(p)\cdot\tilde{x}}.$$

Thus

$$\begin{aligned}E_{ij}^{(0)}&=\big\{2\big(\mathrm{i}\kappa_j^{(1)}(p)\big)\big(\mathrm{i}\kappa_i^{(1)}(p)\big)\hat{\phi}(p)\\&\quad+\big[\big(\mathrm{i}\kappa_j^{(2)}(p)\big)\big\{\big(\mathrm{i}\kappa^{(2)}(p)\big)\times\hat{\psi}(p)\big\}_i\\&\quad+\big(\mathrm{i}\kappa_i^{(2)}(p)\big)\big\{\big(\mathrm{i}\kappa^{(2)}(p)\big)\times\hat{\psi}(p)\big\}_j\big]\big\}e^{\mathrm{i}\alpha(p)\cdot\tilde{x}}\\&=-\big\{2\big(\kappa_j^{(1)}(p)\big)\big(\kappa_i^{(1)}(p)\big)\mathcal{L}_\phi\big[\hat{\xi}(p)\big]\\&\quad+\big[\big(\kappa_j^{(2)}(p)\big)\big\{\big(\kappa^{(2)}(p)\big)\times\mathcal{L}_\psi\big[\hat{\xi}(p)\big]\big\}_i\\&\quad+\big(\kappa_i^{(2)}(p)\big)\big\{\big(\kappa^{(2)}(p)\big)\times\mathcal{L}_\psi\big[\hat{\xi}(p)\big]\big\}_j\big]\big\}e^{\mathrm{i}\alpha(p)\cdot\tilde{x}},\end{aligned}$$

and, for $n>0$,

$$\begin{aligned}E_{ij}^{(n)}&=F_n\big\{2\big(\mathrm{i}\gamma^{(1)}(p)\big)^n\big(\mathrm{i}\kappa_j^{(1)}(p)\big)\big(\mathrm{i}\kappa_i^{(1)}(p)\big)\hat{\phi}(p)\\&\quad+\big(\mathrm{i}\gamma^{(2)}(p)\big)^n\big[\big(\mathrm{i}\kappa_j^{(2)}(p)\big)\big\{\big(\mathrm{i}\kappa^{(2)}(p)\big)\times\hat{\psi}(p)\big\}_i\\&\quad+\big(\mathrm{i}\kappa_i^{(2)}(p)\big)\big\{\big(\mathrm{i}\kappa^{(2)}(p)\big)\times\hat{\psi}(p)\big\}_j\big]\big\}e^{\mathrm{i}\alpha(p)\cdot\tilde{x}}\\&=-F_n\big\{2\big(\mathrm{i}\gamma^{(1)}(p)\big)^n\big(\kappa_j^{(1)}(p)\big)\big(\kappa_i^{(1)}(p)\big)\mathcal{L}_\phi\big[\hat{\xi}(p)\big]\\&\quad+\big(\mathrm{i}\gamma^{(2)}(p)\big)^n\big[\big(\kappa_j^{(2)}(p)\big)\big\{\big(\kappa^{(2)}(p)\big)\times\mathcal{L}_\psi\big[\hat{\xi}(p)\big]\big\}_i\\&\quad+\big(\kappa_i^{(2)}(p)\big)\big\{\big(\kappa^{(2)}(p)\big)\times\mathcal{L}_\psi\big[\hat{\xi}(p)\big]\big\}_j\big]\big\}e^{\mathrm{i}\alpha(p)\cdot\tilde{x}}.\end{aligned}$$

References

[1] J.D. Achenbach, Wave Propagation in Elastic Solids, North-Holland, Amsterdam, 1973.
[2] J. Billingham, A.C. King, Wave Motion, Cambridge Texts in Applied Mathematics, Cambridge University Press, Cambridge, 2000.
[3] M. Bouchon, A review of the discrete wavenumber method, Pure Appl. Geophys. 160 (3) (2003) 445–465.
[4] Oscar P. Bruno, Fernando Reitich, Numerical solution of diffraction problems: a method of variation of boundaries, J. Opt. Soc. Am. A 10 (6) (1993) 1168–1175.
[5] Oscar P. Bruno, Fernando Reitich, Numerical solution of diffraction problems: a method of variation of boundaries. II. Finitely conducting gratings, Padé approximants, and singularities, J. Opt. Soc. Am. A 10 (11) (1993) 2307–2316.
[6] Oscar P. Bruno, Fernando Reitich, Numerical solution of diffraction problems: a method of variation of boundaries. III. Doubly periodic gratings, J. Opt. Soc. Am. A 10 (12) (1993) 2551–2562.
[7] Oscar P. Bruno, Fernando Reitich, Calculation of electromagnetic scattering via boundary variations and analytic continuation, Appl. Comput. Electromagn. Soc. J. 11 (1) (1996) 17–31.
[8] Oscar P. Bruno, Fernando Reitich, Boundary-variation solutions for bounded-obstacle scattering problems in three dimensions, J. Acoust. Soc. Am. 104 (5) (1998) 2579–2583.
[9] Florian Bleibinhaus, Stéphane Rondenay, Effects of surface scattering in full-waveform inversion, Geophysics 74 (6) (2009) WCC69–WCC77.
[10] J.M. Chesneaux, A.A. Wirgin, Response to comments on "Reflection from a corrugated surface revisited", J. Acoust. Soc. Am. 98 (1995) 1815–1816.
[11] R. Coifman, M. Goldberg, T. Hrycak, M. Israeli, V. Rokhlin, An improved operator expansion algorithm for direct and inverse scattering computations, Waves Random Media 9 (3) (1999) 441–457.
[12] David Colton, Rainer Kress, Inverse Acoustic and Electromagnetic Scattering Theory, second edition, Springer-Verlag, Berlin, 1998.
[13] R. Coifman, Y. Meyer, Nonlinear harmonic analysis and analytic dependence, in: Pseudodifferential Operators and Applications, Notre Dame, Ind., 1984, Amer. Math. Soc., 1985, pp. 71–78.
[14] Craig Walter, Catherine Sulem, Numerical simulation of gravity waves, J. Comput. Phys. 108 (1993) 73–83.
[15] J.J. Greffet, C. Baylard, P. Versaevel, Diffraction of electromagnetic waves by crossed gratings: a series solution, Opt. Lett. 17 (1992) 1740–1742.
[16] D. Givoli, Recent advances in the DtN FE method, Arch. Comput. Methods Eng. 6 (2) (1999) 71–116.
[17] F. Gilbert, L. Knopoff, Seismic scattering from topographic irregularities, J. Geophys. Res. 65 (10) (1960) 3437–3444.
[18] J.J. Greffet, Z. Maassarani, Scattering of electromagnetic waves by a grating: a numerical evaluation of the iterative-series solution, J. Opt. Soc. Am. A 7 (1990) 1483–1493.

[19] David Gottlieb, Steven A. Orszag, Numerical analysis of spectral methods: theory and applications, in: CBMS-NSF Regional Conference Series in Applied Mathematics, vol. 26, Society for Industrial and Applied Mathematics, Philadelphia, PA, 1977.
[20] C. Godrèche (Ed.), Solids Far from Equilibrium, Cambridge University Press, Cambridge, 1992.
[21] J.J. Greffet, Scattering of electromagnetic waves by rough dielectric surfaces, Phys. Rev. B 37 (1988) 6436–6441.
[22] I. Herrera, A perturbation method for elastic wave propagation: 1. Nonparallel boundaries, J. Geophys. Res. 69 (18) (1964) 3845–3851.
[23] E.Y. Harper, F.M. Labianca, Perturbation theory for scattering of sound from a point source by a moving rough surface in the presence of refraction, J. Acoust. Soc. Am. 57 (1975) 1044–1051.
[24] E.Y. Harper, F.M. Labianca, Scattering of sound from a point source by a rough surface progressing over an isovelocity ocean, J. Acoust. Soc. Am. 58 (1975) 349–364.
[25] Bei Hu, David P. Nicholls, Analyticity of Dirichlet–Neumann operators on Hölder and Lipschitz domains, SIAM J. Math. Anal. 37 (1) (2005) 302–320.
[26] Frank Ihlenburg, Finite Element Analysis of Acoustic Scattering, Springer-Verlag, New York, 1998.
[27] D.R. Jackson, D.P. Winebrenner, A. Ishimaru, Comparison of perturbation theories for rough-surface scattering, J. Acoust. Soc. Am. 83 (1988) 961–969.
[28] L. Kazandjian, Comparison of the Rayleigh–Fourier and extinction theorem methods applied to scattering and transmission at a rough solid–solid interface, J. Acoust. Soc. Am. 92 (1992) 1679–1691.
[29] K. Koketsu, H. Fujiwara, Y. Ikegami, Finite-element simulation of seismic ground motion with a voxel mesh, J. Pure Appl. Geophys. 161 (11–12) (2004).
[30] Joseph B. Keller, Dan Givoli, Exact nonreflecting boundary conditions, J. Comput. Phys. 82 (1) (1989) 172–192.
[31] D. Komatitsch, J. Tromp, Spectral-element simulations of global seismic wave propagation—I. Validation, Geophys. J. Int. 149 (2) (2002) 390–412.
[32] D. Komatitsch, J. Tromp, Spectral-element simulations of global seismic wave propagation—II. 3-D models, oceans, rotation, and self-gravitation, Geophys. J. Int. 150 (1) (2002) 303–318.
[33] C. Lopez, F.J. Yndurain, N. Garcia, Iterative series for calculating the scattering of waves from hard corrugated surfaces, Phys. Rev. B 18 (1978) 970–972.
[34] D. Michael Milder, An improved formalism for rough-surface scattering of acoustic and electromagnetic waves, in: Proceedings of SPIE – The International Society for Optical Engineering, San Diego, 1991, vol. 1558, Int. Soc. for Optical Engineering, Bellingham, WA, 1991, pp. 213–221.
[35] D. Michael Milder, An improved formalism for wave scattering from rough surfaces, J. Acoust. Soc. Am. 89 (2) (1991) 529–541.
[36] D. Michael Milder, An improved formalism for electromagnetic scattering from a perfectly conducting rough surface, Radio Sci. 31 (6) (1996) 1369–1376.
[37] D. Michael Milder, Role of the admittance operator in rough-surface scattering, J. Acoust. Soc. Am. 100 (2) (1996) 759–768.
[38] Alison Malcolm, David P. Nicholls, Operator expansions and constrained quadratic optimization for interface reconstruction: impenetrable acoustic media, Wave Motion 51 (2014) 23–40.
[39] P. Moczo, J.O.A. Robertsson, L. Eisner, The finite-difference time-domain method for modeling of seismic wave propagation, Adv. Geophys. 48 (2007) 421.
[40] D. Michael Milder, H. Thomas Sharp, Efficient computation of rough surface scattering, in: Mathematical and Numerical Aspects of Wave Propagation Phenomena, Strasbourg, 1991, SIAM, Philadelphia, PA, 1991, pp. 314–322.
[41] D. Michael Milder, H. Thomas Sharp, An improved formalism for rough surface scattering. II: Numerical trials in three dimensions, J. Acoust. Soc. Am. 91 (5) (1992) 2620–2626.
[42] A.H. Nayfeh, O.R. Asfar, Parallel-plate waveguide with sinusoidally perturbed boundaries, J. Appl. Phys. 45 (1974) 4797–4800.
[43] David P. Nicholls, Traveling water waves: spectral continuation methods with parallel implementation, J. Comput. Phys. 143 (1) (1998) 224–240.
[44] David P. Nicholls, Efficient enforcement of far-field boundary conditions in the transformed field expansions method, J. Comput. Phys. 230 (22) (2011) 8290–8303.
[45] David P. Nicholls, Fernando Reitich, A new approach to analyticity of Dirichlet–Neumann operators, Proc. R. Soc. Edinb. A 131 (6) (2001) 1411–1433.
[46] David P. Nicholls, Fernando Reitich, Stability of high-order perturbative methods for the computation of Dirichlet–Neumann operators, J. Comput. Phys. 170 (1) (2001) 276–298.
[47] David P. Nicholls, Fernando Reitich, Analytic continuation of Dirichlet–Neumann operators, Numer. Math. 94 (1) (2003) 107–146.
[48] David P. Nicholls, Fernando Reitich, Shape deformations in rough surface scattering: cancellations, conditioning, and convergence, J. Opt. Soc. Am. A 21 (4) (2004) 590–605.
[49] David P. Nicholls, Fernando Reitich, Shape deformations in rough surface scattering: improved algorithms, J. Opt. Soc. Am. A 21 (4) (2004) 606–621.
[50] R. Gerhard Pratt, Frequency-domain elastic wave modeling by finite differences: a tool for crosshole seismic imaging, Geophysics 55 (5) (1990) 626–632.
[51] Rayleigh Lord, On the dynamical theory of gratings, Proc. R. Soc. Lond. A 79 (1907) 399–416.
[52] S.O. Rice, Reflection of electromagnetic waves from slightly rough surfaces, Commun. Pure Appl. Math. 4 (1951) 351–378.
[53] J. Roginsky, Derivation of closed-form expressions for the T matrices of Rayleigh–Rice and extinction-theorem perturbation theories, J. Acoust. Soc. Am. 90 (1991) 1130–1137.
[54] Roel Snieder, The influence of topography on the propagation and scattering of surface waves, Phys. Earth Planet. Inter. 44 (3) (1986) 226–241.
[55] F.J. Sanchez-Sesma, E. Perez-Rocha, Diffraction of elastic waves by three-dimensional surface irregularities. Part II, Bull. Seismol. Soc. Am. 79 (1) (1989) 101.
[56] J. Virieux, S. Operto, An overview of full-waveform inversion in exploration geophysics, Geophysics 74 (6) (2009) WCC1–WCC26.
[57] Alexander G. Voronovich, Wave Scattering from Rough Surfaces, second edition, Springer-Verlag, Berlin, 1999.
[58] J.R. Wait, Perturbation analysis for reflection from two-dimensional periodic sea waves, Radio Sci. 6 (1971) 387–391.
[59] J.H. Woodhouse, F.A. Dahlen, The effect of a general aspherical perturbation on the free oscillations of the Earth, Geophys. J. R. Astron. Soc. 53 (2) (1978) 335–354.
[60] Ru-Shan Wu, The perturbation method in elastic wave scattering, in: Scattering and Attenuation of Seismic Waves, Part II, Springer, 1989, pp. 605–637.
[61] O.C. Zienkiewicz, The Finite Element Method in Engineering Science, 3rd ed., McGraw-Hill, New York, 1977.